energies

MDPI

Article

Leveraging Prosumer Flexibility to Mitigate Grid Congestion in Future Power Distribution Grids

Domenico Tomaselli [1,2,*], Dieter Most [3], Enkel Sinani [4], Paul Stursberg [1], Hans Joerg Heger [1] and Stefan Niessen [2,3]

[1] Technology, Sustainable Energy and Infrastructure, Siemens AG, 81739 Munich, Germany; paul.stursberg@siemens.com (P.S.); hans-joerg.heger@siemens.com (H.J.H.)
[2] Department of Electrical Engineering and Information Technology, Technical University of Darmstadt, 64287 Darmstadt, Germany; stefan.niessen@siemens.com
[3] Technology, Sustainable Energy and Infrastructure, Siemens AG, 91058 Erlangen, Germany; dieter.most@siemens.com
[4] School of Computation, Information and Technology, Technical University of Munich, 85748 Munich, Germany; enkel.sinani@tum.de
* Correspondence: domenico.tomaselli@siemens.com

Abstract: The growing adoption of behind-the-meter (BTM) photovoltaic (PV) systems, electric vehicle (EV) home chargers, and heat pumps (HPs) is causing increased grid congestion issues, particularly in power distribution grids. Leveraging BTM prosumer flexibility offers a cost-effective and readily available solution to address these issues without resorting to expensive and time-consuming infrastructure upgrades. This work evaluated the effectiveness of this solution by introducing a novel modeling framework that combines a rolling horizon (RH) optimal power flow (OPF) algorithm with a customized piecewise linear cost function. This framework allows for the individual control of flexible BTM assets through various control measures, while modeling the power flow (PF) and accounting for grid constraints. We demonstrated the practical utility of the proposed framework in an exemplary residential region in Schutterwald, Germany. To this end, we constructed a PF-ready grid model for the region, geographically allocated a future BTM asset mix, and generated tailored load and generation profiles for each household. We found that BTM storage systems optimized for self-consumption can fully resolve feed-in violations at HV/MV stations but only mitigate 35% of the future load violations. Implementing additional control measures is key for addressing the remaining load violations. While curative measures, e.g., temporarily limiting EV charging or HP usage, have minimal impacts, proactive measures that control both the charging and discharging of BTM storage systems can effectively address the remaining load violations, even for grids that are already operating at or near full capacity.

Keywords: behind-the-meter assets; flexibility; smart grid; grid congestion; optimal power flow

Citation: Tomaselli, D.; Most, D.; Sinani, E.; Stursberg, P.; Heger, H.J.; Niessen, S. Leveraging Prosumer Flexibility to Mitigate Grid Congestion in Future Power Distribution Grids. *Energies* **2024**, *17*, 4217. https://doi.org/10.3390/en17174217

Academic Editor: Federico Barrero

Received: 12 July 2024
Revised: 7 August 2024
Accepted: 20 August 2024
Published: 23 August 2024

1. Introduction

1.1. Motivation

Europe has set ambitious climate targets, aiming to install 600 GW of PV capacity, double the deployment of HPs, and achieve a 30% market share of EVs by 2030 [1]. This transformation, primarily occurring at the BTM level, is adding significant stress to power distribution grids, leading to grid congestion, which often manifests as equipment overloading and can accelerate grid degradation [2–5].

To address grid congestion and consistently deliver high-quality, uninterrupted power to supplied end consumers, distribution system operators (DSOs) often implement infrastructure upgrades. However, these upgrades are capital-intensive, particularly if they occur before the existing equipment has reached the end of its service life. Moreover, they are

time-consuming on a large scale, potentially lagging behind the rapid adoption of BTM assets [6].

On the other hand, this transformation creates a new category of BTM prosumers. Leveraging the flexibility of these prosumers can present a cost-effective and readily available solution for mitigating grid congestion [7]. To investigate the effectiveness of this solution, we introduce an integrated approach, which models the future power distribution grid in a specific region and evaluates the potential of BTM prosumer flexibility and various control measures to effectively mitigate grid congestion issues.

1.2. Related Work

Levering flexibility to mitigate grid congestion issues is attracting significant research interest. The authors of [8] explored five different flexibility options and evaluated their capacity to reduce the need for grid infrastructure upgrades from a techno-economic perspective. In [7], the authors introduce a framework for procuring prosumer flexibility, enabling DSOs to mitigate the need for grid expansion measures. Similar concepts were also investigated in [9,10]. A study [11] suggests that implementing control strategies for flexible BTM assets can effectively prevent grid congestion. Our work builds upon this study by integrating a power distribution grid and analyzing a large section of a system (more than 300 households), rather than focusing only on individual households.

Geographic information system (GIS)-based approaches have been previously used for energy system modeling. The FlexiGIS platform, as proposed in [12], leverages the spatial data extracted from open-source databases, e.g., OpenStreetMap, to optimize flexibility option costs and operation in urban areas. This platform has also been used in [13,14] for optimal battery storage allocation. While these works did not consider the power distribution grid, this aspect was addressed in the comprehensive GIS-based study proposed in [15]. Our approach builds upon this study by integrating rooftop PVs, EV home chargers, and battery and thermal storage alongside HPs.

To model the behavior and management of prosumer flexibility, several approaches, including OPF-based algorithms, have been proposed. A study [16] proposes an OPF-based algorithm to optimize flexible asset scheduling within microgrids. The concept of flexibility in microgrids was also investigated in [17] using, however, mixed integer linear programming (MILP). In [18], the authors present an approach for integrating sizing, placement, and operational strategies for battery storage into OPF. This concept was further investigated in [19], taking into account various penetration levels of wind power and load scales, and in [20] using MILP and mixed integer nonlinear programming.

1.3. Contributions

In this paper, we present a novel approach for assessing how BTM prosumer flexibility can mitigate grid congestion issues in future power distribution grids. To this end, we determined the future BTM asset mix for a specific region and geographically allocated the assets to the households. We used existing algorithms and tools as well as open-source data to collect and prepare the necessary input data. This included constructing a PF-ready grid model of the existing infrastructure and generating tailored load demand and generation profiles for each household. We introduce a modeling framework that uses an RH OPF algorithm to control flexible BTM assets over time without perfect foresight while considering grid constraints.

We applied the proposed approach in a case study of a residential region in Schutterwald, Germany. This study shows that the approach can quantify the impact of future BTM asset penetration on grid congestion issues with minimal input data. We then analyzed these issues and evaluate various control measures for flexible BTM assets to identify the most effective solutions.

The remainder of the paper is structured as follows: The proposed approach is presented in Section 2. The simulation experiments are outlined in Section 3. In Section 4,

we summarize the results, discuss the limitations, and present potential avenues for future work.

2. Materials and Methods

The proposed approach comprises three key parts. First, the BTM asset mix is determined for both a status quo and a future scenario. Second, the input data required for the proposed modeling framework are collected and prepared. Third, the modeling framework for controlling BTM prosumer flexibility is applied. Note that the approach, graphically described in Figure 1, is automated and transferrable to different regions with similar infrastructure. Moreover, it is versatile for different data availability scenarios, e.g., if the actual grid model and/or measurements are available, they can be directly used.

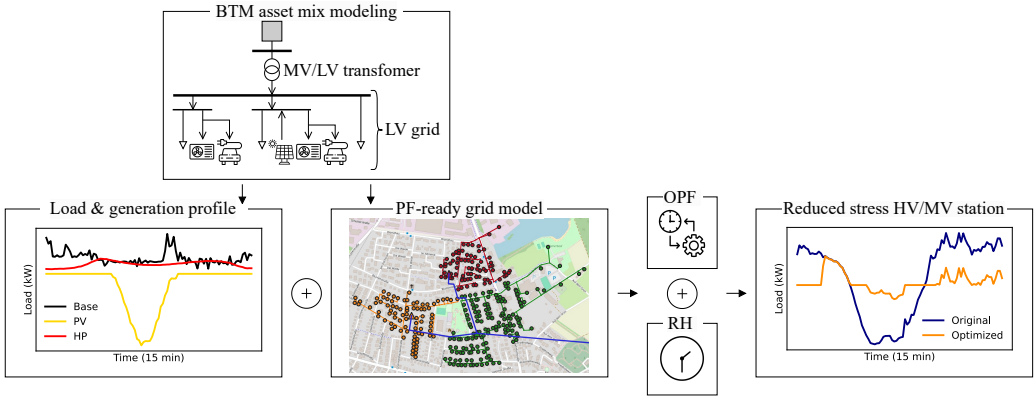

Figure 1. Schematic describing the workflow of the proposed approach.

2.1. Status Quo and Future Behind-the-Meter Asset Mix

When determining the BTM asset mix for a specific region, we considered two different scenarios: one for the status quo (year 2024) and another for the future (year 2030).

In the status quo scenario, we considered rooftop PVs as the only type of BTM asset. We assumed a 25% penetration rate, reflecting the current level of rooftop PV adoption in Schutterwald, Germany. Based on this rate, we randomly selected households behind each MV/LV station and geographically allocated the rooftop PVs. We determined this scenario to estimate the status quo load on the HV/MV station, which was then used to establish the threshold for grid congestion detection (Section 3.1).

In the future scenario, we used a more generalized approach, integrating a wider range of BTM assets, i.e., rooftop PVs, Level 2 EV home chargers, HPs, and both battery and thermal storage. These assets vary in their degree of flexibility, as outlined in Table 1. Battery and thermal storage are fully flexible, allowing complete control by the OPF algorithm within the modeling framework. EV home chargers and HPs are partially flexible, i.e., temporary reductions in their usage can be enforced when necessary. Household load and rooftop PVs, on the other hand, have a fixed electric load or generation profile.

Table 1. Summary of the BTM asset mix for the future scenario.

Asset Type	Flexibility Level	Avg. Penetration	MV/LV Station (No. Households)		
			Reference	Focus PV	Focus EV
Household load	Fixed	100%	85	157	77
Rooftop PV	Fixed	47%	39	73	46
EV charger (Level 2)	Partial	26%	17	51	15
Heat pump	Partial	40%	34	62	30
Battery storage	Full	47%	39	73	46
Thermal storage	Full	19%	17	22	19

The projected penetration rates of each asset were extrapolated from the targets established in the REPowerEU plan [1]. Similar to the status quo scenario, we randomly

selected households behind each MV/LV station based on these penetration rates and geographically allocated the assets to the households. Note that in this work, battery storage systems were only allocated to households with a rooftop PV, whereas thermal storage systems were only allocated to households with both a rooftop PV and HP.

To increase the diversity of the future BTM asset mix, we slightly varied the projected penetration rates of rooftop PVs and EV home chargers at two out of the three available MV/LV stations. Precisely, one MV/LV station ("Focus PV" in Table 1) shows an increased trend in rooftop PV adoption of 60%, while another MV/LV station ("Focus EV" in Table 1) experiences a higher installation rate of EV home chargers of 33%. The remaining MV/LV station ("Reference" in Table 1) represents the projected average penetration rates. The details of the future scenario are summarized in Table 1.

2.2. Input Data

In the following, we outline the procedures for collecting and preparing the input data for the application of the proposed modeling framework.

2.2.1. Generating a Grid Model for Power Flow Simulations

We considered an exemplary residential region in Schutterwald, Germany, comprising one 25 MVA HV/MV station, two 0.63 MVA MV/LV stations, one 0.4 MVA MV/LV station, and 319 households.

The locations and nameplate capacities of the HV/MV station and the MV/LV stations were extracted from the open-source MV-Oberrhein power grid available in [21]. We obtained the locations and living areas of the households using a custom extension for the Overpass API [22] developed in Python 3.10, which automatically fetches information from OpenStreetMap [23] based on the region's coordinates.

Since we assumed that detailed information about the LV power grid is not available, we used the algorithm from [24] to produce a synthetic estimate of the system (Figure 2). The generated power grid was assumed to represent the existing infrastructure. While it may not precisely align with the actual system, it serves as the benchmark for applying the proposed modeling framework. To explicitly account for uncertainty, this procedure can be also extended to generate a probability distribution including several potential candidates.

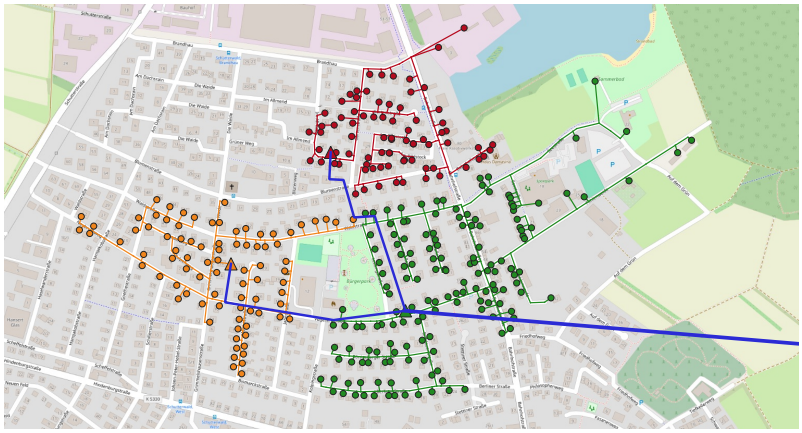

Figure 2. The grid model used for the experiments, shown on a geographical map. This system includes the LV power grid estimated in this work and the MV power grid from [21] supplying it.

We generated the synthetic estimate as follows:

Step 1. Using the custom extension for Overpass API, we automatically fetched the street layout of the region.

Step 2. We construcedt a network of the region by linking the street layout with the nearest node of the MV/LV stations and households. Then, we eliminated all redundant nodes, e.g., additional nodes of the MV/LV stations and households

that were not connected to the street layout. In the following, this network is referred to as the base graph.

Step 3. We applied the approach proposed in [24] to produce a possible assignment of the end consumers to the available MV/LV stations while adhering to the base graph.

Step 4. We derived the grid topology by applying a minimum spanning tree algorithm and pruning all edges not leading to a household or MV/LV station node, as proposed in [24].

Step 5. We developed a PF-ready grid model by specifying the technical parameters for the grid assets using pandapower [21].

2.2.2. Household Load and Generation Profiles

We used an automated approach to create load and generation profiles with configurable granularity tailored to the households to which they were geographically assigned. In this work, all load and generation profiles are configured with a 15-minute granularity. Similarly to Section 2.2.1, the application of this approach was necessary since we assumed that actual measurements are not available. However, if measured profiles for all households are available, this step can be omitted, and the measured profiles can be used instead.

Electric Base Load Profiles

We relied on an open-source dataset, featuring exemplary German energy consumption profiles from [25], to produce the electric base load profiles for individual households as of today. To this end, for each household $i \in \{1, \ldots, N\}$, where N is the total number of households, we randomly selected a profile from [25] and normalized it according to its inherent total energy consumption. Then, we scaled the resulting normalized profile by adapting the formula provided in the context of [26] for dimensioning residential household energy consumption

$$E_i = E_{\text{avg}} \times \frac{A_i}{A_{\text{avg}}} \tag{1}$$

where E_{avg} is the average residential energy consumption in Germany, A_i is the living area of a household i, and A_{avg} is the average residential living area in Germany. Finally, we derived the electric base load profiles for the individual households by transforming the estimated energy consumption data into load profiles.

Thermal Base Load Profiles

To generate the thermal load profiles, we adopted an approach similar to the one outlined in the previous paragraph. First, we derived the normalized thermal load profile for the region of interest using NASA's MERRA-2 weather dataset [27] and the methodology introduced in [28]. Then, for each household i with living area A_i, we assumed compliance with the Efficiency House 40 standard [29] and adjusted the normalized profile by a factor of 40 $\text{kWh}_{\text{thermal}}$ / $\text{m}^2 \times A_i$. Finally, we introduced slight random fluctuations and temporal shifts to each resulting profile to reduce cross-correlation effects between households. Note that a thermal load profile was only generated for households equipped with HPs. Moreover, the resulting thermal load profile represents a household's requirements for space heating and hot water generation rather than the operation of the HP.

Electric Generation Profiles

We determined the generation data for the region of interest by using NASA's MERRA-2 weather dataset [27] and identifying key parameters, e.g., incident irradiance on PV modules and temperature influences, as described in [30]. After normalizing the resulting generation data, we adjusted it according to a predefined PV capacity. For simplicity, we assumed that all households within the region of interest had rooftop PVs with 6.6 kW PV capacity in the status quo scenario and 8 kW PV capacity in the future scenario.

Electric Vehicle Charging Profiles

We used the agent-based modeling approach proposed in [31] to generate the profiles for all households equipped with EV home chargers. The charging capacity is adjustable; though, for simplicity, we assumed that all residential EV chargers within the region of interest have a uniform maximum power of 11 kW.

2.3. Modeling Framework

The proposed modeling framework (see the flowchart in Figure 3) consists of four key components, described in more detail in the subsections below: (1) modeling of BTM battery and thermal storage systems over time, (2) an RH OPF algorithm equipped with a customized piecewise linear cost function for flexible BTM asset control, (3) curative control measures for EV home chargers and HPs, and (4) proactive control measures for BTM storage systems. The framework was developed in Python 3.10, primarily leveraging the pandapower and Pandas libraries. Its design is highly modular, allowing each component to operate as a standalone module that can be used independently or in conjunction with others.

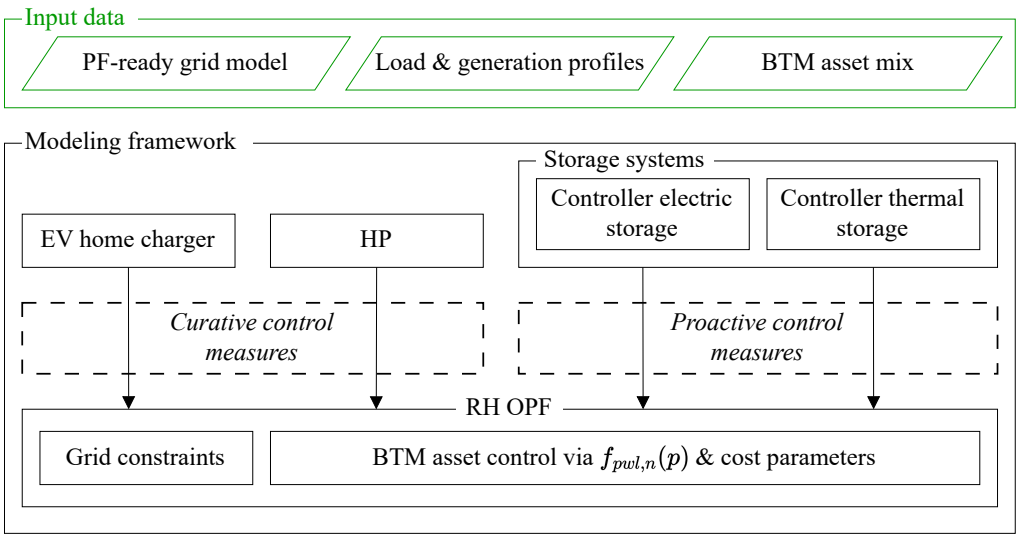

Figure 3. Flowchart describing the input data and workflow of the proposed modeling framework.

Note that while AC OPF is supported, we used DC OPF in this study due to its significantly shorter runtime. Moreover, we evaluated the load at the HV/MV station using both AC OPF and DC OPF over an exemplary one-week period. We found that the load simulated with AC OPF is generally slightly higher than that simulated using DC OPF. However, the discrepancy is negligible, i.e., less than 5%.

2.3.1. Modeling of Storage Systems

In this work, we considered a BTM system (Figure 4) that included both battery and thermal storage systems. While pandapower can fundamentally model a storage system, it does not dynamically update its state of charge (SOC) during power flow calculations. We addressed this limitation by developing a control module that updates the SOC, as well as the charging and discharging power for both the battery and thermal storage at each time step along the RH.

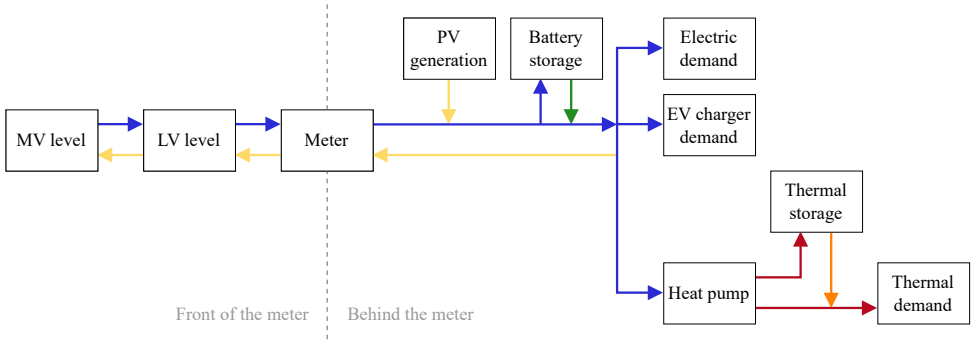

Figure 4. Schematic of the BTM system considered in this work, showing the flow of the supplied (——), fed-in (——), and stored (——) electric power, as well as the supplied (——) and stored (——) thermal power.

Let $E_{\text{stor, cap}}$ be the capacity of a storage system and $p_{\text{stor}}(t)$ be its power (positive when charging and negative when discharging) at timestamp t. We calculate the SOC of the storage system at timestamp t as

$$SOC(t) = SOC(t-1) + \left[\frac{E_{\text{stor}}(t-1) + (\Delta t * p_{\text{stor}}(t))}{E_{\text{stor,cap}}}\right], \quad (2)$$

where $E_{\text{stor}}(t-1)$ is the energy remaining in the storage system from the previous timestamp, and Δt is the length of a timestamp, e.g., $\Delta t = 0.25$ for input data with 15-min granularity.

The charging and discharging powers of a storage system are initially set as predefined fixed values. However, if a storage system is nearing depletion during the RH, i.e., $E_{\text{stor}}(t) \leq \Delta t * p_{\text{stor}}(t)$, the discharging power is adjusted to $min(1/\Delta t * E_{\text{stor}}(t), p_{\text{stor}}(t))$. In contrast, if a storage system is nearing full capacity, i.e., $E_{\text{stor}}(t) \geq E_{\text{stor, cap}} - (\Delta t * p_{\text{stor}}(t))$, then the charging power is adjusted to $1/\Delta t * (E_{\text{stor, cap}} - E_{\text{stor}}(t))$.

While the control module for battery storage is straightforward, developing one for thermal storage requires more extensive work. As can be seen in Figure 4, we used the HP as the interface between the thermal and electric loads of a household, making it the only asset capable of charging thermal storage. Moreover, during discharge, the thermal storage is specifically tailored to exclusively address the thermal load demand.

To model these functionalities, we synchronized the maximum charging power of the thermal storage with the thermal power of the HP. Then, during discharge, we dynamically calculated an upper bound based on the current thermal load demand. Note that the conversion of thermal load to electric load was achieved using the time-dependent coefficient of performance (COP), which was determined for the region of interest using ambient temperature data and the methodology introduced in [28]. This conversion is inherent in the developed control module of thermal storage and is key for correctly updating its SOC.

In this work, we considered 16 $\text{kWh}_{\text{electric}}$ lithium-ion battery storage systems for storing electric energy from rooftop PVs or the grid, along with 11.6 $\text{kWh}_{\text{thermal}}$ thermal storage tanks (the thermal storage capacity was derived from an assumed volume of 1000 L for the water tank) for storing thermal energy from the HPs.

2.3.2. Behind-the-Meter Control of Flexible Assets

To control flexible BTM assets, we made two key assumptions: First, both battery and thermal storage optimize self-consumption [32]. Second, due to the higher versatility of battery storage, which can supply multiple electric BTM assets including HPs, we prioritized charging battery storage before thermal storage. On the other hand, when discharging, thermal storage is discharged before battery storage.

To establish this control strategy with OPF, we define a piecewise linear cost function $f_{\text{pwl},n}(p)$ and cost parameters for the power p supplied by the grid and the storage systems

(see Table 2). Since an HP is used for charging thermal storage, the actual charging costs of thermal storage include both the operational costs of the HP and the direct costs associated with charging the thermal storage. Note that the cost parameters do not represent actual real-world energy costs. Instead, they were virtual values used exclusively to establish a control strategy of the flexible assets. Moreover, in the context of an RH, the defined cost parameters generally remain constant over time but can be dynamically adjusted, e.g., for implementing proactive control measures (Figure 5). Given the defined cost parameters, the OPF algorithm optimizes $f_{\text{pwl},n}(p)$ at each timestamp along the RH as

$$min \sum_{n \in \{\text{grid, battery storage, thermal storage}\}} f_{\text{pwl},n}(p) \quad (3)$$

while accounting for grid constraints. A flowchart describing the workflow of the proposed RH OPF algorithm is shown in Figure 5.

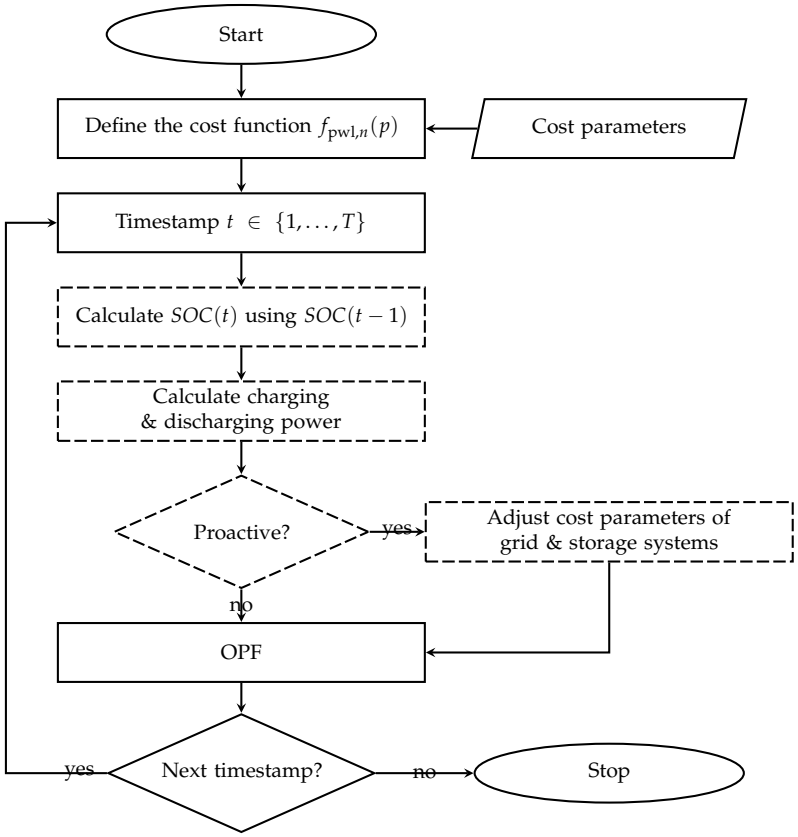

Figure 5. Flowchart describing the workflow of the proposed RH OPF algorithm for simulations over T timestamps. The dashed blocks (**- - -**) represent the additions introduced in this work.

Table 2. Cost parameters used to control BTM storage systems using the RH OPF algorithm.

Asset	Mode	Cost Parameter
Grid	Feed-in Load	−0.7 0.7
Battery storage	Charge Discharge	0.2 −0.6
Heat pump (HP)	Load	0.25
Thermal storage	Charge Discharge	0.04 −0.04

2.3.3. Modeling the Curative Control Measures

We implemented two curative control measures based on the guidelines outlined in § 14a EnWG, which allow DSOs in Germany to reactively (1) reduce EV charging or (2) reduce HP usage up to 4.2 kW per controllable unit.

These measures were implemented as follows. Based on a day-ahead forecast at the HV/MV station, we first identified potential grid congestion and determined the critical hours. Since an actual forecast was not available in the context of this work, we used a pseudo-forecast derived from performing a PF simulation of the future scenario without BTM storage systems.

If congestion is identified in the forecast, then the first curative measure, denoted as CurA, reduces the maximum charging power of all EV home chargers in the region from 11 kW to 3.7 kW starting from the onset of the identified issue until the end of the day. Let $t_0 \in \{1, \ldots, T_{\text{day}}\}$ be the first timestamp in the day-ahead forecast where grid congestion is identified. Let p_{EV} be the load profile of an EV home charger during this period, with a total charging energy of E_{EV}. We calculate the controlled charging profile $p_{\text{EV, CurA}}$ for all timestamps $t \in \{1, \ldots, T_{\text{day}}\}$ as

$$p_{\text{EV, CurA}}(t) = \begin{cases} p_{\text{EV}}(t) & \text{if } t < t_0 \\ 3.7 \text{ kW} & \text{if } t_0 \leq t \leq T_{\text{day}} \end{cases}. \tag{4}$$

If the controlled EV charging profile does not satisfy the total required charging energy by the end of the day, i.e., $E_{\text{EV}} > \Delta t * \sum_{t_0 \leq t \leq T_{\text{day}}} 3.7 \text{ kW}$, then the remaining load is charged at the start of the next day using the original charging power, e.g., see Figure 6 (Top).

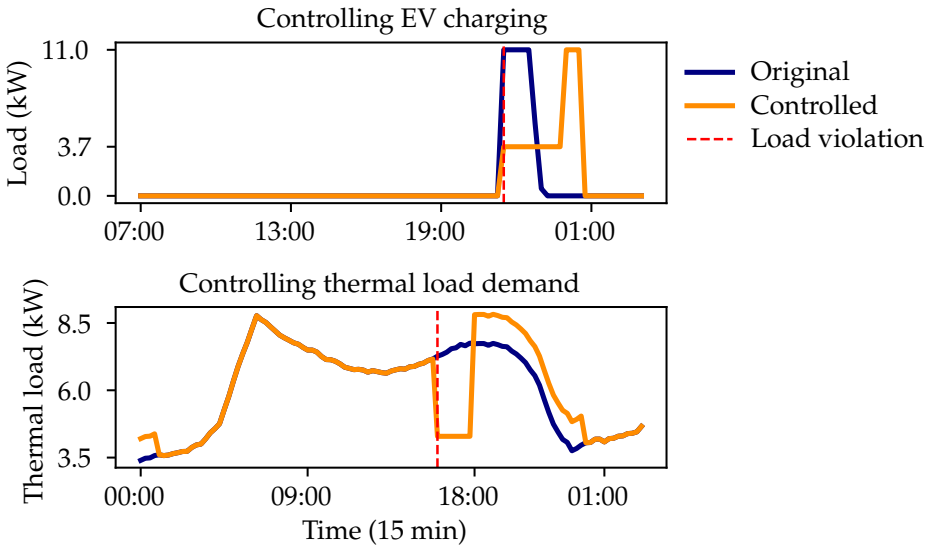

Figure 6. Curative control measures. (**Top**) CurA reduces the original EV charging value to a predefined minimum power during periods of forecasted grid congestion. This approach requires longer charging times to compensate for the deferred energy. (**Bottom**) CurB reduces the original thermal load demand signal during periods of forecasted grid congestion, but an increased thermal load is required afterward to compensate for the deferred energy.

The second curative measure, denoted as CurB, temporarily reduces HP usage to 30% of its maximum capacity for two hours [33] from the onset of the congestion period. Let p_{thermal} be the thermal load profile of a household during grid congestion with maximum

thermal power $p_{\text{thermal, max}}$ and total energy E_{thermal}. We calculate the controlled thermal load demand signal $p_{\text{thermal, CurB}}$ for all timestamps $t \in \{1, \ldots, T_{\text{day}}\}$ as

$$p_{\text{thermal, CurB}}(t) = \begin{cases} p_{\text{thermal}}(t) & \text{if } t < t_0 \\ 0.3 * p_{\text{thermal, max}} & \text{if } t_0 \leq t \leq T_{2\text{h}} \end{cases}, \tag{5}$$

where $T_{2\text{h}} \in \{1, \ldots, T_{\text{day}}\}$ is the last timestamp of the two-hour interval starting from t_0 during which CurB is deployed.

After this interval, the deferred thermal energy, i.e., $E_{\text{thermal}} - \Delta t * \sum_{t_0 \leq t \leq T_{2\text{h}}} 0.3 * p_{\text{thermal, max}}$, is compensated within the next six hours (an official compensation time is not specified in § 14a EnWG; the six-hour duration used in this study is an estimated assumption), e.g., see Figure 6 (Bottom).

Note that the settings of both curative measures can be adjusted.

2.3.4. Modeling the Proactive Control Measures

Two proactive control measures were investigated in this work. The first measure, denoted as ProA, involves proactively charging the BTM storage systems. The second measure, denoted as ProB, involves controlled discharging of the BTM storage systems. The two measures can be applied individually or together. In this work, we considered two scenarios: (1) ProA only and (2) both ProA and ProB.

Conceptually, these measures follow a similar approach to the curative control measures described in Section 2.3.3. Regarding ProA, we first identify grid congestion in the day-ahead forecast and extract the critical hours. Then, we define the grid cost parameter $c_{\text{grid}}(t)$ for a suitable time interval $T_{\text{charge}} \subset \{1, \ldots, T_{\text{day}}\}$ (a time interval before the start of the identified grid congestion where the load on the HV/MV station is also expected to be low) as

$$c_{\text{grid, ProA}}(t) = \begin{cases} 0.0 & \text{if } t \in T_{\text{charge}} \\ c_{\text{grid}}(t) & \text{else} \end{cases} \tag{6}$$

to enable the charging of BTM storage systems ahead of the identified grid congestion, even when PV generation is insufficient, see, e.g., Figure 7 (Top).

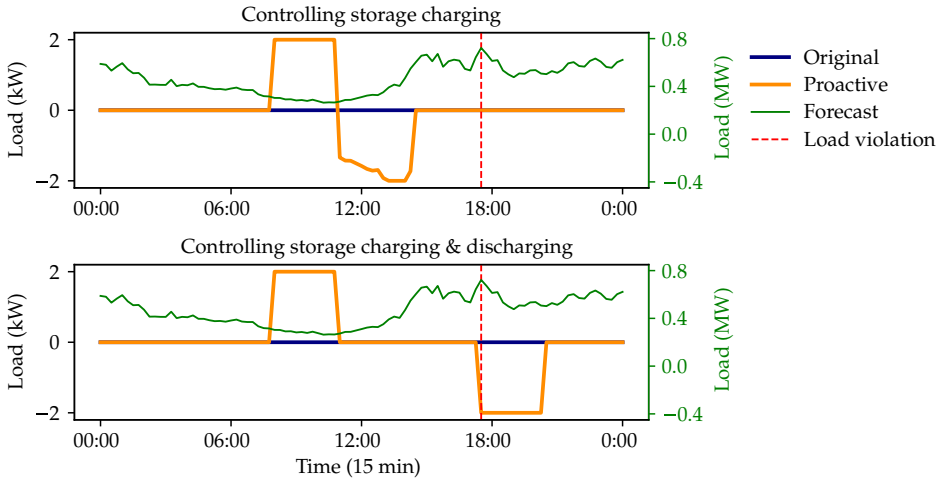

Figure 7. Proactive control measures. (**Top**) ProA increases the charging capacity of the storage systems before a forecasted grid congestion. (**Bottom**) ProA and ProB increase the charging capacity before forecasted grid congestion and start discharging at the onset of the congestion period.

Regarding ProB, we define the discharge cost parameter of the storage systems $c_{\text{stor, discharge}}(t)$ for all timestamps $t \in \{1, \ldots, T_{\text{day}}\}$ as

$$c_{\text{stor, discharge, ProB}}(t) = \begin{cases} -1.0 & \text{if } t < t_0 \\ c_{\text{stor, discharge}}(t) & t_0 \leq t \leq T_{\text{day}} \end{cases} \quad (7)$$

to start discharging the BTM storage systems at the start of the identified grid congestion, e.g., see Figure 7 (Bottom).

To implement these measures within the modeling framework, a control module that updates the grid cost parameters over time was developed and integrated into the RH OPF algorithm, see Figure 5. Moreover, the functionality of the control modules for BTM storage systems was extended to include the adjustment of the storage discharge cost parameters over time.

3. Results

In the following, we demonstrate how leveraging BTM prosumer flexibility with appropriate control measures can successfully mitigate grid congestion in future power distribution grids. First, we assessed the impact of transitioning from the status quo BTM asset mix to the future BTM asset mix with the existing infrastructure. Using the proposed modeling framework, we then investigated six different scenarios of flexible BTM asset control to address the identified grid congestion issues.

All experiments were performed using a standard Lenovo laptop equipped with an Intel i7-12800H CPU.

3.1. Grid Congestion Detection

In this work, we focused on detecting grid congestion in the form of overloading at the HV/MV station level. Given that we only considered three MV/LV stations behind the HV/MV station and the actual HV/MV station supplies many more, we could not determine the overload threshold based on its specified nameplate capacity. Instead, we derived it from the maximum peak load of the HV/MV station under current conditions. We calculated this load by performing a PF simulation based on the settings and generated profiles of the status quo scenario. The rationale for using this threshold for the future scenario was to ensure that the load on the HV/MV station remained consistent with today's level despite the projected increase of BTM assets.

As future violations depend on the peak stress level at which the grid is currently operating, we distinguished between three different levels for detecting overloading: (1) *safe* (a grid in the specified region operating today up to 90% of the allowed limit), (2) *near-critical* (up to 95%), and (3) *critical* (up to 100%).

This distinction was achieved by adjusting the previously described threshold based on the margin between the status quo peak load and the capacity of the HV/MV substation.

3.2. Future BTM Asset Mix Impact on Today's Power Distribution Grid

To investigate the impact of the future BTM asset mix on today's power distribution grid, we performed a PF simulation and identify grid congestion issues, as outlined in Section 3.1.

Figure 8a,b show the identified load and feed-in violation instances throughout the year and day for a grid critically stressed today. As can be seen, load violations predominantly occur during winter months in the evening or late at night. This can be attributed to the surge in power used as people return home in the evenings, as well as potential EV charging and increased demand for heating in winter. On the other hand, feed-in violations primarily occur around mid-day and during spring and summer due to the increased PV generation and the lack of flexible BTM assets to absorb the excess generated energy.

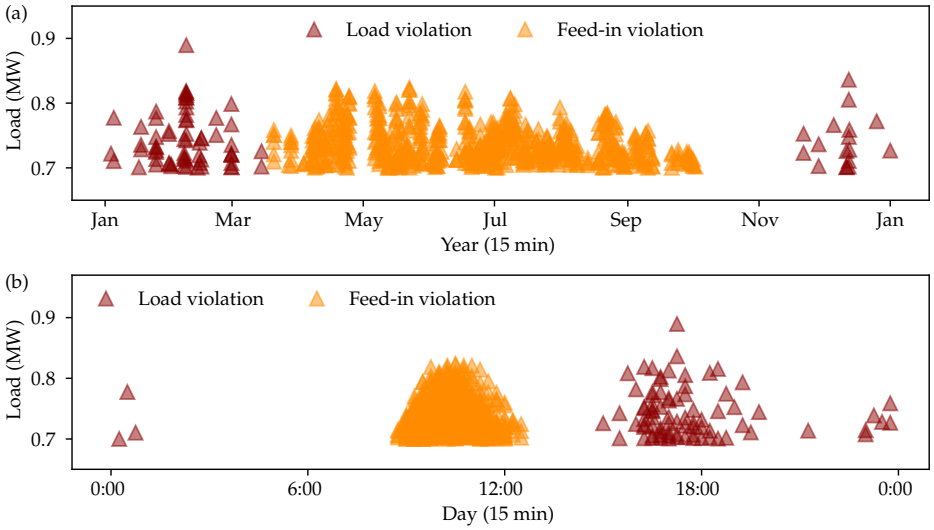

Figure 8. Instances of (**a**) annual and (**b**) daily loads and feed-in violations identified for a grid critically stressed today when subjected to the BTM asset mix in the future scenario.

These findings are further substantiated in Figure 9 (red bars), which shows the count of 15 min intervals with either load or feed-in violations at the HV/MV station throughout the year. As evident, several load and feed-in violations are likely in 2030 if the grid is already critically stressed today. The count reduces as the margin between the status quo peak load and the capacity of the substation increases.

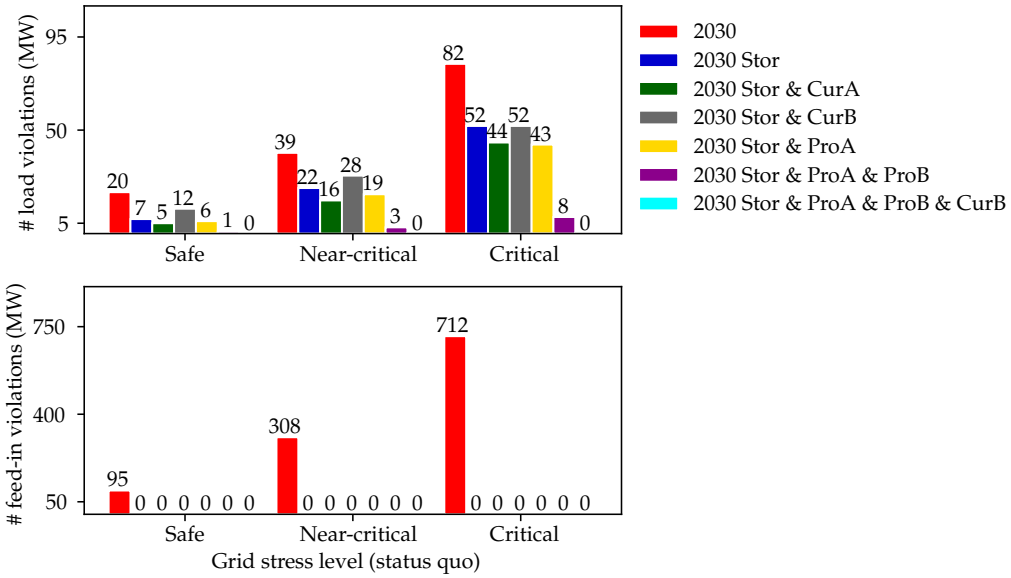

Figure 9. Annual count of load and feed-in violations at the HV/MV station for all six scenarios of flexible BTM asset control (storage denoted as Stor, curative denoted as Cur, and proactive denoted as Pro).

3.3. BTM Storage Systems

In the first scenario of flexible BTM asset control, ws incorporate both battery and thermal storage systems. In the following, we refer to this scenario as the 2030 Stor scenario.

As shown in Figure 9 (blue bars), integrating storage systems effectively mitigates feed-in violations and decreases the frequency of load violations substantially, e.g., by 35% for a grid critically stressed today. This improvement can be partially attributed to the high penetration rate and large capacity of the battery storage systems considered in this

work, which we expect to be available by 2030. However, storage systems alone do not completely mitigate all load violations. During the winter months, when PV generation is low, these assets are scarcely charged. Moreover, since we assumed that they are operated using self-consumption optimization, they discharge as soon as the electricity demand exceeds the current generation of the rooftop PVs. Particularly with low charging, this mechanism can lead to storage systems being depleted before the evening and night peak hours, when the grid is more likely to experience overload.

3.4. BTM Storage Systems with Curative Control Measures

In the second and third scenarios of flexible BTM asset control, we attempted to address the remaining load violations in the 2030 Stor scenario by implementing curative measures that temporarily restrict EV charging or HP usage.

As evident in Figure 9, CurA (green bars) marginally improves overloading, while CurB (gray bars) has a negligible impact and, in cases where the grid is safe or near-critical, can even be detrimental. The limited improvement resulting from controlling EV charging can be attributed to its low aggregated impact on the HV/MV station. This is due to two main factors: First, the projected penetration rate of EV home chargers is lower compared to that of other BTM assets. Second, multiple EV charging events rarely coincide to the same extent as, e.g., with HP usage. Note that this impact may change when considering public charging stations.

While limiting EV charging has a marginal yet positive impact on overload, Figure 10 demonstrates how restricting HP usage during forecasted peak hours can aggravate overloading. As can be seen, implementing this control measure successfully reduces grid stress during the two designated hours when the HPs operate at a lower capacity. The deferred thermal load demand, however, is compensated by running the HPs with higher capacities over the following six hours (cold load pickup), often creating several load violations that did not previously occur.

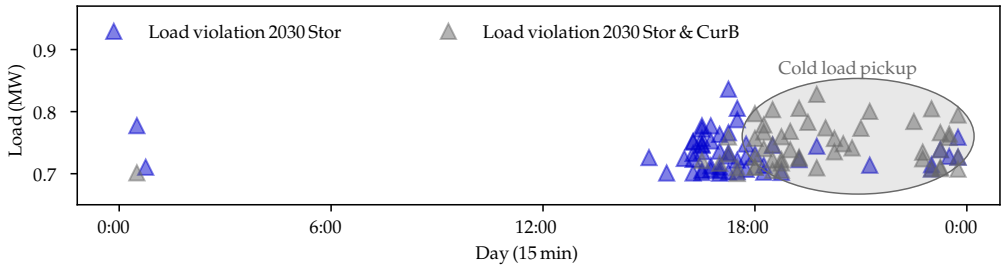

Figure 10. Annual number of load violations in 2030 for a grid critically stressed today, comparing scenarios with storage systems only and with both storage systems and CurB.

3.5. BTM Storage Systems with Proactive Control Measures

Since curative measures only marginally mitigate the remaining load violations in the 2030 Stor scenario, we attempted to resolve them by implementing different combinations of proactive control measures in the last scenarios of flexible BTM asset control.

As shown in Figure 9, implementing ProA alone (gold bars) has a marginal impact. This is because the BTM storage systems continue to optimize self-consumption, leading to their depletion before the load violation occurs.

In contrast, the combination of ProA and ProB—where both the charging and discharging of the BTM storage systems are controlled—effectively eliminates nearly all identified load violations in the 2030 Stor scenario, see Figure 9 (purple bars). Even for grids that are critically stressed today, the combination of both proactive measures can resolve up to 90% of the identified load violations.

Proactive Control Measures with Controlled HP Usage

Figure 9 shows that even by integrating both proactive control measures, a few load violations persist for grids operating at or near critical stress levels today. These violations primarily occur at night-time, mainly due to heating demands.

As shown in Section 3.4, we found that while CurB is ineffective in reducing load violations on its own, it can successfully address night-time (after 23:00) load violations. During this time, HPs can operate at higher capacity due to the reduced household load, allowing the deferred thermal load demand to be compensated without causing additional violations. As a result, integrating CurB with ProA and ProB eliminates all load violations across all three grid stress levels, see Figure 9 (cyan bars).

4. Conclusions

In this work, we investigated the potential of BTM prosumer flexibility for mitigating grid congestion issues in future power distribution grids.

To achieve this, we introduced a modeling framework that employs an RH OPF algorithm and a customized piecewise linear cost function to control flexible BTM assets of individual prosumers over time without perfect foresight, while accounting for grid constraints. This framework is part of an integrated approach that also includes constructing a PF-ready grid model for a specific region, determining the future BTM asset mix for 2030, geographically allocating these assets to households and generating tailored load and generation profiles for each household. This approach is versatile and can be applied in different data availability scenarios. When the actual grid model and measurements are available, they are directly used. If this information is missing, as in this work, the approach can still be applied to provide preliminary estimates of the future stress on the grid and assess the potential of BTM prosumer flexibility to mitigate identified grid congestion issues.

We applied the proposed approach to an example of a residential region in Schutterwald, Germany, comprising an HV/MV station, three MV/LV stations, and 319 households. Our findings suggest that BTM storage systems optimized for self-consumption are not sufficient for mitigating future stress on power distribution grids. Precisely, while integrating BTM storage systems can mitigate feed-in violations, only 35% of the detected load violations are resolved in a grid that is critically stressed today. To avoid costly and time-consuming infrastructure upgrades on a large scale, additional control measures can be implemented. Curative control measures based on the guidelines in § 14a EnWG that limit EV charging and HP usage have a minimal impact, i.e., resolving, respectively, an additional 11% and 1% of the detected load violations when implemented alongside BTM storage systems. On the other hand, proactive measures that control the charging and discharging of BTM storage systems can effectively address the remaining load violations, especially when combined with reduced HP usage to mitigate load violations at night-time.

To summarize, this paper introduced the following:

(1) A novel approach for evaluating how BTM prosumer flexibility can address grid congestion issues in a specific region, using an RH OPF algorithm and a customized piecewise linear cost function.
(2) We modeled both the battery and, for the first time to the best of our knowledge, thermal storage systems as flexible BTM assets controllable by the RH OPF algorithm.
(3) The key conclusions derived from applying the proposed approach are as follows: (a) BTM storage systems alone are insufficient to mitigate grid congestion issues in future power distribution grids, (b) curative measures based on existing guidelines have minimal impacts, and (c) proactive measures controlling both the charging and discharging of BTM storage systems are necessary to effectively address these issues.

4.1. Discussion and Limitations

In this work, we demonstrated that grid congestion issues in future power distribution grids can be addressed by leveraging BTM prosumer flexibility. While long-term infrastructure upgrades will likely still be necessary, the proposed measures for controlling flexible

BTM assets offer a valuable short-term solution. Precisely, the implementation of these measures can provide DSOs with additional time to upgrade the existing infrastructure, potentially postponing these upgrades until the end of the service life of the grid equipment, thereby saving significant investment costs.

This study focused on the growing adoption of rooftop PVs, Level 2 EV home chargers, HPs, and storage systems. However, new relevant BTM assets may emerge in the future, e.g., air conditioning systems. The modular design of our approach supports the integration of additional BTM assets, which can be seamlessly incorporated into the BTM asset control algorithm by designing appropriate cost parameters.

Moreover, the components of the proposed approach can be exchanged if necessary. For example, while our approach is based on pandapower, it can be adapted to other power system modeling tools, provided they offer a comparable OPF algorithm that supports the proposed modeling framework.

The input data used in this work were synthesized from open-source information specific to a single region. The results may vary when using real-world data and considering regional differences, e.g., the structure and operation of a balanced European-style grid differ from those of an asymmetric USA-style grid. To validate the universal applicability of our approach, additional experiments using real-world data from various regions are necessary.

The proposed control measures for mitigating grid congestion rely on (1) the widespread adoption of BTM storage systems and (2) the willingness of prosumers to engage in these measures. The latter point is particularly important and deserves further discussion, as it may affect residents' quality of life.

During periods of grid congestion, EV home chargers may charge more slowly, and buildings may experience reduced heating as HPs are temporarily operated at reduced capacity. Moreover, storage systems no longer optimize self-consumption, with discharging starting only at the onset of grid congestion. As a result, any energy needed by the residents prior to grid congestion must be supplied by the grid and billed accordingly. This raises questions about how to motivate prosumers to engage in these control measures. One potential solution would be to subsidize the installation of BTM storage systems in grids critically stressed today and include a contract clause requiring the prosumers to participate in the control measures.

4.2. Future Work

There are several avenues for future work. We are actively engaged in expanding the grid congestion assessment and analysis of the HV/MV station. The power distribution grid considered in this work was synthetic and modeled after a European-style system. It would be interesting to migrate the proposed framework to other grid types, e.g., USA-style grids, as well as real-world grids. Moreover, the focus of this study was exclusively on single-family households that were uniform in age and energy refurbishment. It would be also interesting to include different residential household types, e.g., multifamily households with different ages and energy refurbishments, as well as commercial buildings, and determine their impact on HV/MV stations. We plan to enhance the current assignment of BTM assets, demands, and demand profiles to households by implementing a more sophisticated approach that reflects different characteristics of the buildings. Finally, we used a pseudo-forecast when implementing the control measures. Integrating a proper forecasting approach and accounting for the uncertainty that comes with the forecast are also worth investigating.

Author Contributions: Conceptualization, D.T., D.M., E.S., P.S., and H.J.H.; methodology, D.T., D.M., and E.S.; software, D.T. and E.S.; validation, D.M., P.S., and H.J.H.; formal analysis, D.M., D.T., and E.S.; data curation, D.T.; visualization, D.T.; writing—original draft preparation, D.T., writing—review and editing, D.M., H.J.H., P.S., and S.N.; supervision, D.M., P.S., H.J.H., and S.N. All authors have read and agreed to the published version of this manuscript.

Funding: This research received no external funding.

Data Availability Statement: The original contributions presented in the study are included in the article, further inquiries can be directed to the corresponding authors.

Acknowledgments: We would like to extend our gratitude to Hakan Özlemis for his valuable contributions to the development of the method presented in this paper.

Conflicts of Interest: The authors Domenico Tomaselli, Dieter Most, Paul Stursberg, Hans Jörg Heger and Stefan Niessen were employed by the Siemens AG. The remaining authors declare that the research was conducted in the absence of any commercial or financial relationships that could be construed as a potential conflict of interest.

Abbreviations

The following abbreviations are used in this manuscript:

PV	Photovoltaic
EV	Electric vehicle
HP	Heat pump
BTM	Behind-the-meter
DSO	Distribution system operator
GIS	Geographic information system
HV	High voltage
MV	Medium voltage
LV	Low voltage
PF	Power flow
OPF	Optimal power flow
RH	Rolling horizon
AC	Alternating current
DC	Direct current
COP	Coefficient of performance
API	Application programming interface

References

1. Commision, E. Renewable Energy Targets. 2023. Available online: https://energy.ec.europa.eu/topics/renewable-energy_en (accessed on 22 May 2024)
2. Cossent, R.; Gómez, T.; Frías, P. Towards a future with large penetration of distributed generation: Is the current regulation of electricity distribution ready? Regulatory recommendations under a European perspective. *Energy Policy* **2009**, *37*, 1145–1155. [CrossRef]
3. van der Welle, A.J.; de Joode, J. Regulatory road maps for the integration of intermittent electricity generation: Methodology development and the case of The Netherlands. *Energy Policy* **2011**, *39*, 5829–5839. [CrossRef]
4. Pepermans, G.; Driesen, J.; Haeseldonckx, D.; Belmans, R.; D'haeseleer, W. Distributed generation: Definition, benefits and issues. *Energy Policy* **2005**, *33*, 787–798. [CrossRef]
5. *IEEE Standard C57.91-2011*; Guide for Loading Mineral-Oil-Immersed Transformers and Step-Voltage Regulators. Institute of Electrical and Electronics Engineers: New York, NY, USA, 2011.
6. Commision, E. Grids, the missing link—An EU Action Plan for Grids. 2023. Available online: https://eur-lex.europa.eu/legal-content/EN/TXT/?uri=COM%3A2023%3A757%3AFIN&qid=1701167355682 (accessed on 22 May 2024).
7. Spiliotis, K.; Gutierrez, A.I.R.; Belmans, R. Demand flexibility versus physical network expansions in distribution grids. *Appl. Energy* **2016**, *182*, 613–624. [CrossRef]
8. Resch, M.; Bühler, J.; Schachler, B.; Sumper, A. Techno-economic assessment of flexibility options versus grid expansion in distribution grids. *IEEE Trans. Power Syst.* **2021**, *36*, 3830–3839. [CrossRef]
9. Ramos, A.; De Jonghe, C.; Gómez, V.; Belmans, R. Realizing the smart grid's potential: Defining local markets for flexibility. *Util. Policy* **2016**, *40*, 26–35. [CrossRef]
10. Esmat, A.; Usaola, J.; Moreno, M.Á. Distribution-level flexibility market for congestion management. *Energies* **2018**, *11*, 1056. [CrossRef]
11. Pfleger, J.; Medved, T.; Zupančič, J.; Gubina, A.F.; Lakić, E. Modelling of flexibility options in a low voltage distribution system. In Proceedings of the 2022 18th International Conference on the European Energy Market (EEM), Ljubljana, Slovenia, 13–15 September 2022; pp. 1–5.
12. Alhamwi, A.; Medjroubi, W.; Vogt, T.; Agert, C. FlexiGIS: An open source GIS-based platform for the optimisation of flexibility options in urban energy systems. *Energy Procedia* **2018**, *152*, 941–946. [CrossRef]

13. Alhamwi, A.; Medjroubi, W.; Vogt, T.; Agert, C. GIS-based urban energy systems models and tools: Introducing a model for the optimisation of flexibilisation technologies in urban areas. *Appl. Energy* **2017**, *191*, 1–9. [CrossRef]
14. Alhamwi, A.; Medjroubi, W.; Vogt, T.; Agert, C. Development of a GIS-based platform for the allocation and optimisation of distributed storage in urban energy systems. *Appl. Energy* **2019**, *251*, 113360. [CrossRef]
15. Kisse, J.M.; Braun, M.; Letzgus, S.; Kneiske, T.M. A GIS-Based planning approach for urban power and natural gas distribution grids with different heat pump scenarios. *Energies* **2020**, *13*, 4052. [CrossRef]
16. Grover-Silva, E.; Heleno, M.; Mashayekh, S.; Cardoso, G.; Girard, R.; Kariniotakis, G. A stochastic optimal power flow for scheduling flexible resources in microgrids operation. *Appl. Energy* **2018**, *229*, 201–208. [CrossRef]
17. Khederzadeh, M. Defining and realizing flexibility in distribution grid. In Proceedings of the CIRED Workshop 2016, Helsinki, Finland, 14–15 June 2016; pp. 1–4.
18. Grover-Silva, E.; Girard, R.; Kariniotakis, G. Optimal sizing and placement of distribution grid connected battery systems through an SOCP optimal power flow algorithm. *Appl. Energy* **2018**, *219*, 385–393. [CrossRef]
19. Qin, M.; Chan, K.W.; Chung, C.Y.; Luo, X.; Wu, T. Optimal planning and operation of energy storage systems in radial networks for wind power integration with reserve support. *IET Gener. Transm. Distrib.* **2016**, *10*, 2019–2025. [CrossRef]
20. Spiliotis, K.; Claeys, S.; Gutierrez, A.R.; Driesen, J. Utilizing local energy storage for congestion management and investment deferral in distribution networks. In Proceedings of the 2016 13th International Conference on the European Energy Market (EEM), Porto, Portugal, 6–9 June 2016; pp. 1–5.
21. Thurner, L.; Scheidler, A.; Schäfer, F.; Menke, J.H.; Dollichon, J.; Meier, F.; Meinecke, S.; Braun, M. pandapower—An open-source python tool for convenient modeling, analysis, and optimization of electric power systems. *IEEE Trans. Power Syst.* **2018**, *33*, 6510–6521. [CrossRef]
22. Olbricht, R. Overpass API, 2012. Available online: https://wiki.openstreetmap.org/wiki/Overpass_API (accessed on 22 May 2024).
23. OpenStreetMap Contributors. 2017. Available online: https://planet.osm.org (accessed on 22 May 2024).
24. Tomaselli, D.; Stursberg, P.; Metzger, M.; Steinke, F. Representing topology uncertainty for distribution grid expansion planning. In Proceedings of the CIRED 2023, Rome, Italy, 12–15 June 2023; Volume 2023.
25. Tjaden, T.; Bergner, J.; Weniger, J.; Quaschning, V. Representative Electrical Load Profiles of Residential Buildings in Germany with a Temporal Resolution of One Second Dataset HTW Berlin, 2015. Available online: https://www.researchgate.net/publication/285577915_Representative_electrical_load_profiles_of_residential_buildings_in_Germany_with_a_temporal_resolution_of_one_second (accessed on 22 May 2024).
26. Meinecke, S.; Sarajlić, D.; Drauz, S.R.; Klettke, A.; Lauven, L.P.; Rehtanz, C.; Moser, A.; Braun, M. Simbench—A benchmark dataset of electric power systems to compare innovative solutions based on power flow analysis. *Energies* **2020**, *13*, 3290. [CrossRef]
27. Gelaro, R.; McCarty, W.; Suárez, M.J.; Todling, R.; Molod, A.; Takacs, L.; Randles, C.A.; Darmenov, A.; Bosilovich, M.G.; Reichle, R.; et al. The modern-era retrospective analysis for research and applications, version 2 (MERRA-2). *J. Clim.* **2017**, *30*, 5419–5454. [CrossRef] [PubMed]
28. Ruhnau, O.; Hirth, L.; Praktiknjo, A. Time series of heat demand and heat pump efficiency for energy system modeling. *Sci. Data* **2019**, *6*, 189. [CrossRef] [PubMed]
29. Kolb, C. Enegry Transition 2.0. 2024. Available online: https://www.kfw.de/stories/index-en.html (accessed on 22 May 2024).
30. Albrecht, P. *Weiterentwicklung eines Tools zur Analyse der Potentiellen Solar- und Windenergieausbeute Weltweit*; Technical report; Technische Universität München: Munich, Germany, 2016.
31. Husarek, D.; Salapic, V.; Paulus, S.; Metzger, M.; Niessen, S. Modeling the Impact of Electric Vehicle Charging Infrastructure on Regional Energy Systems: Fields of Action for an Improved e-Mobility Integration. *Energies* **2021**, *14*, 7992. [CrossRef]
32. Hirschl, B.; Struth J.; Kairies, K.P.; Leuthold, M.; Aretz A.; Bost M.; Gährs, S.; Cramer, M.; Szczechowicz, E.; Schnettler, A.; Sauer, D.U. PV-benefit: A critical review of the effect of grid integrated PV-storage-systems. In Proceedings of the International Renewable Energy Storage Conference (IRES), Berlin, Germany, 18–20 November 2013.
33. Bundesnetzagentur. Integration von Steuerbaren Verbrauchseinrichtungen. 2024. Available online: https://www.bundesnetzagentur.de/DE/Vportal/Energie/SteuerbareVBE/artikel.htmll (accessed on 22 May 2024).